



GLOBAL JOURNAL OF RESEARCHES IN ENGINEERING: A  
MECHANICAL AND MECHANICS ENGINEERING  
Volume 18 Issue 1 Version 1.0 Year 2018  
Type: Double Blind Peer Reviewed International Research Journal  
Publisher: Global Journals  
Online ISSN:2249-4596 Print ISSN:0975-5861

# Experimental Characterization of Milling, Compaction and Sintering of Nanocrystalline FC-0205 Copper-Steel Powder

By Olalekan R. Junaid, Tonya W. Stone & Jamel H. Alexander

*Mississippi State University*

**Abstract-** The effect of ball milling on the compaction and sintering of nanocrystalline copper steel powder (FC-0205) was evaluated within this work. The as-received micron-sized FC-0205 copper steel powder was subjected to High Energy Ball Milling (HEBM) in an argon atmosphere at different milling times of 0, 16, 20 and 24 hours to obtain nanocrystalline structures. Unmilled, 8 and 16 hours milled powders were compacted using uniaxial die compression at pressures ranging from 274 MPa to 775 MPa to obtain a relative density range of 74% to 95%, respectively. The steel powder compacts were sintered at temperatures ranging from 400 °C to 1120 °C in high purity hydrogen and nitrogen atmospheres. X-ray Diffraction (XRD) and microscopy analysis were performed on the milled powder specimens to evaluate particle size, morphology, and extent of porosity; to establish a relationship between milling time and particle size, and to establish a correlation between grain size and milling time.

**Keywords:** *nanocrystalline powder, ball milling, uniaxial die compaction, sintering, characterization.*

**GJRE-A Classification:** FOR Code: 091399



*Strictly as per the compliance and regulations of:*



# Experimental Characterization of Milling, Compaction and Sintering of Nanocrystalline FC-0205 Copper-Steel Powder

Olalekan R. Junaid<sup>α</sup>, Tonya W. Stone<sup>σ</sup> & Jamel H. Alexander<sup>ρ</sup>

**Abstract-** The effect of ball milling on the compaction and sintering of nanocrystalline copper steel powder (FC-0205) was evaluated within this work. The as-received micron-sized FC-0205 copper steel powder was subjected to High Energy Ball Milling (HEBM) in an argon atmosphere at different milling times of 0, 16, 20 and 24 hours to obtain nanocrystalline structures. Unmilled, 8 and 16 hours milled powders were compacted using uniaxial die compression at pressures ranging from 274 MPa to 775 MPa to obtain a relative density range of 74% to 95%, respectively. The steel powder compacts were sintered at temperatures ranging from 400 °C to 1120 °C in high purity hydrogen and nitrogen atmospheres. X-ray Diffraction (XRD) and microscopy analysis were performed on the milled powder specimens to evaluate particle size, morphology, and extent of porosity; to establish a relationship between milling time and particle size, and to establish a correlation between grain size and milling time. Dilatometry analysis was performed on the compacts to examine the density and phase transformations of the specimens during sintering. As the mill time of the steel powder specimens increased, particle fragmentation increased, which resulted in particle size reduction and increased agglomeration of particles. The grain size of the steel powder specimens decreased as the mill time increased. An increase in density occurred as pressure increased. As temperature increased with mill time, compact density increased.

**Keywords:** nanocrystalline powder, ball milling, uniaxial die compaction, sintering, characterization.

## I. INTRODUCTION

Nanocrystalline materials have experienced significant growth in recent years due to their wide range of applications and impressive physical and mechanical properties they exhibit. Since nanocrystalline materials possess a large number of grain boundaries and are dependent on grain size and distribution, they are superior when compared to conventional coarse-grain materials [1]. Properties include enhanced diffusivity, improved ductility, lower thermal conductivity and increased strength [2]. A nanocrystalline powder is characterized by a structural

length or grain size on the order of 100 nm (0.1 μm) or less [3-4]. They can consist of single crystals of less than 100 nm or of conventionally sized particles composed of a nanocrystalline grain structure.

Materials that have grain sizes in the nanosize range tend to have higher mechanical properties, such as increased strength and hardness as compared to their coarser grained counterparts [5]. Nanosized grains prompt dislocation build up at grain boundaries, hence, making dislocation movement into adjacent grains more difficult. The higher the applied stress needed to move dislocations, the higher the yield strength of the material. The correlation between improved strength characteristics with decreased grain size is captured by the Hall-Petch (HP) relation [6] in equation (1),

$$\sigma_y = \sigma_0 + \frac{K_y}{\sqrt{d}} \quad (1)$$

Where  $\sigma_y$  is the yield strength,  $\sigma_0$  is the lattice friction stress to move individual dislocations,  $K_y$  is a constant (HP slope), and  $d$  is the grain size in diameter. The HP relation implies that yield strength increases with decreasing grain size; however, there is a limit to which the material can be decreased to avoid weakening [7-8]. Experiments on nanocrystalline materials have shown that if the grains reached a critical grain size, typically around 10 nm, an inverse Hall-Petch effect is observed [9-11, 12-14]. As the grain size decreases to approximately 10 nm, grain boundaries tend to slide past one another, which results in a reduction of the material's strength.

There are three main techniques to obtain nanocrystalline structures during powder production which influence the size, shape, microstructure, chemistry, and cost of a material [15]. One method involves ball-milling micron-sized powders to obtain the nanosize powder. Another method uses gas or water atomization from which powder is formed from molten metal using a spray of the droplet, however, this method has a lower particle size limitation of ~1-5 μm [17]. The third method is inert gas condensation which results in no impurities but produces a small output capacity [15, 17, and 18]. Among these techniques, ball milling has proven to be the most cost-effective in the production of nanosized powder [15, 17] and is the production method used in most current research. High Energy Ball

Author  $\alpha$ : Alumnus, Mechanical Engineering, Mississippi State University. e-mail: [lorj11@msstate.edu](mailto:lorj11@msstate.edu)

Author  $\sigma$ : Associate Professor of Mechanical Engineering, Mississippi State University. e-mail: [tstone@me.msstate.edu](mailto:tstone@me.msstate.edu)

Author  $\rho$ : Alumnus, Mechanical Engineering, Mississippi State University. e-mail: [jha105@msstate.edu](mailto:jha105@msstate.edu)

Milling (HEBM) is a type of mechanical milling (MM) technique that is utilized in powder metallurgy (PM) consisting of continuous cold welding, fracturing, and re-welding of powder particles [17].

In 1966, John Benjamin and his colleagues experimented by milling nickel and aluminum powders in an oxidizing atmosphere to form nickel super alloys hardened by oxide dispersion. The experiment showed that repeated fracturing and cold welding during milling exposed new oxide layers on the surface of the particles, which resulted in metal alloying [15-19]. This technique became the genesis of the milling and alloying technique and has since then been extremely useful in many industrial applications. Akhtar *et al.* [17] studied the mechanical milling of iron and copper powder from micrometer size to nanosize particles using HEBM. Within the experiment, mechanical energy was generated through the collision of 0.5-inch hard steel milling balls and the milling vial container in a controlled argon atmosphere. The energy produced caused deformation of the steel powder into nanosize particles. The final particle size, shape, and size distribution were dependent on material property, milling energy/frequency, ball size, and the quantity of ball and powder [15].

Akhtar and Fecht [2, 20] observed that milling time played a significant role in obtaining the nanocrystalline aluminum powder. Brian and Poquillon [15, 22] observed that the energy produced during milling enhanced the interaction between steel powder particles, resulting in plastic deformation, fracturing, and cold welding. Suryanarayana *et al.* [21] found that excessive cold welding of particles greater than 100 nm should be avoided by ensuring a stable point between fracturing and cold welding. Similarly, Joao *et al.* [19] suggested the addition of 1-2wt% of stearic acid which acts as a Process Control Agent (PCA) to avert immoderate cold welding during milling of powder particles. Particle Size, morphology, and agglomeration all contribute to the overall density and mechanical strength of a green compact. The particle size distribution during compaction also determines the level of porosity and homogeneity of the green compact.

Poquillon *et al.* and German [22, 23] reported on the dependence of particle size on the tensile stress of green compacts made from spherical copper powders. Their research discovered that the tensile stress increased as the particle size of the copper powder decreased. Also, the smaller the particle size of the specimen, the higher the fatigue strength due to variation in the stress concentration factor with particle size [24-25]. Mechanical milling has become widely used because of its simplicity and most importantly, cost efficiency compared to other techniques [17]. However, mechanical milling still has its shortcomings

that are yet to be addressed by material engineers and scientists [19-21].

Powder contamination is an issue in mechanical milling. The milling condition, milling time, surface formation, particle size and milling environment all determine the level of contamination of the new powder particles. Possible approaches to reducing contamination are to create a milled environment free of impurities, by ensuring the powder particles are free of impurities, reducing the mill time, and by using a milling vial and ball of similar material to the powdered particles.

Several research engineers and scientists have studied the quantification and modeling of high energy ball milling, but limited success has been achieved. Since the quantification and modeling has not been adequately scoped, production at the industrial-scale is difficult because predicting, controlling and optimization of the process are underdeveloped. Ball milling or mechanical milling is the least expensive method to produce large quantities of nanocrystalline powders [17].

The potential application of nanoscale materials for use as novel structural or functional engineering materials largely depends on the consolidation of nanopowders into bulk nanoscale solids. A central issue in adding nanopowder to engineered parts is the consolidation of the powder into sintered parts with full density and nanogained microstructures [3-4, 9-11, 26]. Nanocrystalline powders are much more difficult to process and handle than powders in the micron size range. Changes in properties are caused by an increase in surface atoms of nanoscale powders as the particle diameter decreases. Production and processing of nanopowders are difficult due to small particle size and high specific surface areas. Nanoscale powders tend to agglomerate, which requires additional processing to de-agglomerate or suspend the powders. The nanopowder consolidation and densification process strongly depend on the state of powder agglomeration.

Consolidation of powders into various shapes are a direct result of cold or hot-pressing techniques. Hot pressing is a technique whereby compaction and sintering of metal powder are done at the same time, however, [27] it is time-consuming. Cold pressing involves the application of pressure on metal powders in a closed shaped die to form a green compact. Vagnon *et al.* [28] reported that compacts formed via hot pressing had higher densities and improved homogeneity. Powder pressing is usually done at ambient room temperature and the compacted sample is called a green compact [15].

The compressibility of green compacts is extensively dependent on the compaction pressure [29]. The pressure reduces the volume and porosity of the

compact powder and increases the density [15]. The amount of pressure needed for compaction of green compacts largely depend on powder characteristics, additives and desired density [22]. Pranav *et al.* [27] found that higher pressures were required to compress powders with coarser particles in comparison to powders that contained fine particles of the same material. Poquillon *et al.* and Sang *et al.* [22, 30] investigated the morphology of iron powder and its impact on compaction behavior. They compacted two different iron powders, one with spherical grains and the other with spongy grains at different pressures ranging from 100 to 350 MPa. Their experimental result showed that the iron spherical powder compacts produced lower density compared to the spongy powder compacts at the same compaction pressure.

Camila and Lirio [31] expanded further on the impact of morphology on the compressibility of steel powders. They observed that during compaction, particles with flattened morphologies had greater deformation capacity on compacts due to their high specific surface areas, which increased the internal friction between particles, ultimately, reducing the compressibility of the compacts. During compaction, particles tend to rearrange thereby reducing spaces and gaps, which leads to an increase in density. The density increases due to the more organized packing of the particles that create contact points between them are referred to as the initial stage of compaction [32]. Cold welding occurs during further application of pressure because forces increase between the contact points of the particles. Plastic deformation occurs in the second stage of compaction. Material deformation takes place at this stage due to the stress between the contact points of the powder particles. The plastic flow of particles increases the stress between powder particle contact points which causes deformation of the material. Density increase is much slower in the second stage because frictional force is higher which hinders the easy movement of material. Conversely density in initial stage increases rapidly because of lower resistance of frictional force. Work hardening of the powder occurs in the third stage because of increase in compaction pressure [22].

Lubricants are necessary during compaction to reduce frictional forces that hinder the free movement of powder particles. Lubricants help to form a uniform distribution of particles during compaction [33]. However, immoderate lubrication can store in interparticle pores thereby preventing a uniform distribution and proper compaction of powder. The green compact is then heated at lower temperatures to remove the lubricants so that it has no effect on the density and strength of the sample [15].

The final stage in the press-sinter approach is to sinter the green compact at a temperature below its

melting point. Sintering of green compacts is essential in that the loosely bounded particles are taken from their green state to higher densified compact parts with enhanced thermal and mechanical properties through metallurgical bonding. There are three processes for sintering; solid-state sintering, liquid-phase sintering and activated sintering [34]. Liquid-sintering of alloy metal powders can be accomplished in one of the two ways; by sintering at temperatures above the melting point of one of the constituent powders or by sintering at temperatures below the melting point of the base powder according to a Fe-Cu phase diagram [34, 35].

Compact shrinkage occurs during sintering due to diffusion thereby reducing space and porosity within the sample. Vagnon *et al.* [28] studied the effect of sintering on swelling and shrinkage of steel powder. They observed shrinkage within the steel powders at lower temperatures during the removal of the lubrication. However, at higher sintering temperatures, the copper diffused into the iron thereby causing the compact to swell and reduce in shrinkage. Also, during sintering, recrystallization of atoms, grain growth, and phase change were all noticed [36].

Sintering parameters [29, 37] affect the strength, density and grain size of the of the sintered compact. These parameters include sintering temperature, material composition, powder morphology, time and atmosphere. [17, 28]. Nanocrystalline powders densify at sintering temperatures significantly lower than conventional powders. Densification typically occurs at 0.2 to 0.4 times the melting temperature ( $T_m$ ) as compared to 0.5 to 0.8  $T_m$  for conventional powders [38].

Several researchers have studied the effects of sintering time and temperatures on the mechanical properties of metallic powders. Akhtar *et al.* [2] studied the effects of sintering on steel powders and reported a 50% increase in grain size from the initial powder post-compaction, sintering, and annealing at elevated temperatures. Pranav *et al.* [27] investigated the sintering mechanisms of molybdenum powder and reported that less sintering work was required to achieve the same densification at higher compaction pressures than at lower compaction pressures. Narasimhan [34] stated that metallic powder type and desired geometry determine both sintering time and temperature. He performed an experiment on several alloying elements and concluded that Fe-B-C has the potential to undergo higher sintering temperature than Fe-Cu-C due to the low solubility of boron in iron as compared to copper. Therefore, Fe-B-C can be used in the production of hard steels.

Sintering atmosphere is also a key factor in the sintering process of metal powders [29, 37]. The sintering atmosphere should be controlled to prevent oxidation and unwanted chemical reactions, eliminate

existing oxides and control carburization and decarburization. [37]. Several types of sintered atmospheres are used in powder metallurgy; however, the method in which the atmosphere is controlled during sintering is consequential in relation to the strength of the green compact. The sintering atmosphere is usually controlled with hydrogen, argon, helium, nitrogen, or under vacuum [27, 34]. Previous studies have shown that sintering in a hydrogen environment results in better mechanical properties than under vacuum [37]. Depending on the sintering time and temperature, powder particles start to bond together by forming necks throughout the diffusion process. These necks grow at the points of particle contact and as sintering time increases the neck size ratio increases which help to increase the mechanical strength [37]. At elevated temperatures and increased time, grain growth was noticeable, and pores became spherical and isolated [36]. Vagnon *et al.* [28] postulated two methods to reduce sintering temperature to minimize the growth of grains. They suggested a small amount of elements such as Ni, Pt, Pd, and Co be added to the base powder to activate the sintering process thereby reducing the sintering temperature and time. Nevertheless, the addition of some of these elements with the base powder can reduce the ductility of the sintered sample thereby affecting the mechanical properties. The researchers [37] also stated that nanosize particles require higher compaction pressures at lower sintering times and temperature for grain growth reduction.

This experimental study establishes a correlation between milling time, particle size, temperature and grain growth through HEBM on copper steel powder. The aim of this work was to characterize the structure-property relations of ball-milled nanocrystalline FC-0205 copper steel powder with Ancorsteel 1000B as the base Fe powder; analyze the morphology of powder particles from different milling times and how that particle size affects the density and mechanical properties of the green compact; and lastly, analyze the effects of ball milling on powder consolidation into dense compacts using uniaxial die compression and sintering. The FC-0205 powder system was chosen due to its widespread use in the powder metallurgy industry for automotive applications. The study utilizes a press-sintering technique using uniaxial die compaction followed by sintering.

## II. EXPERIMENTAL PROCEDURES

### a) Milling

As-received copper steel powder FC-0205 mixed with 0.6% zinc stearate lubricant, also known as Acrawax from Hoeganaes was used for this study. Table 1 summarizes the nominal chemical composition of the

as-received iron powder. The prefix (F) designates an iron-based material and the second prefix (C) is copper, which is known as the primary alloying element. The first two digits (02) represent the percentage of the primary alloying element which is 2% copper. Carbon content is represented by the third and fourth digits whereby 05 designates the amount of carbon in a range between 0.3%-0.6%. The base iron powder for FC-0205 is an Ancorsteel 1000B alloy mix commonly used in the powder metallurgy industry. The chemical composition of Ancorsteel 1000B is provided in Table 2.

Table 1: The nominal chemical composition of the as-received FC-0205 iron powder

MPIF designation/Component	Fe	C	Cu	Acrawax
FC-0205	97.1	0.5	2	0.6

Table 2: Ancorsteel 1000B chemical composition by wt%

	Fe	C	O	N	S	P	Si	Mn	Cr	Cu	Ni
Ancorsteel 1000B	Bal.	<0.01	0.09	0.001	0.009	0.005	<0.01	0.1	0.03	0.05	0.05

The as-received FC-0205 powder was milled by Union Process at intervals of 0,8,16, 20 and 24 hours. The milling process was carried out in a Model SD-1 Laboratory Attritor with 6.35 mm (0.25 inch) stainless steel grinding media. A ball-to-powder ratio of 16/1 was used, and the milling speed was set to 350 RPM in a sealed argon environment to lessen the contamination of oxygen and humidity. The stearic acid lubricant was added to the milling process to reduce friction, minimize die wear, aid in the part ejection, and avoid cold welding of the materials. The material properties of the final components are unaffected by the lubricant since the lubricant is burned off before sintering.

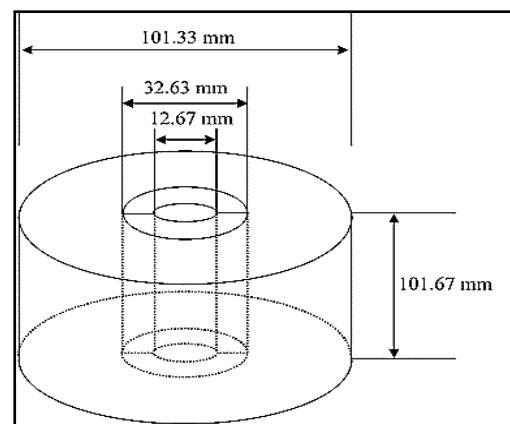


Figure 1: Die Compact

### b) Compaction

Uniaxial cold pressing was performed on the milled and unmilled FC-0205 copper steel powder each.

The shaped die used for compaction and sintering was made of Vasco Max C-350 and had an inner diameter of 32.63 mm (1.3 inches), and an outer diameter of 101.33mm (4 inches) as shown in Figure 1. A cylindrical split hollow die with a diameter of 12.67 mm (0.5 inches) was made of the same material for easy removal of the sample after compaction. An Instron 5882 mechanical test frame with 100 kN load cell was used to exert a compressive force on the shaped die at a constant compression rate of 10 mm/min in a controlled environment. The steel powder was filled into the shaped die, and the upper punch compressed the powder at various heights to achieve different densities. Density measurements were taken before sintering.

#### c) Dilatometer Tests

A vertical push rod dilatometer (Anter Corporation Unitherm Model 1161) was used for the dilatometry analysis to examine the density and phase transformations of the unmilled samples during sintering. FC-0205 compacts were heated to 1150 °C (2102 °F) in a nitrogen atmosphere at different heating rates (2C/min, 5C/min, and 10C/min). The samples were held for 30 minutes followed by an uncontrolled cool down from the sintering cycle. Dilatometry measurements were captured when the push rod attached to a transducer displaced with the shrinkage or expansion of the compact. The signals obtained from the motion transducer and thermocouple were correlated by a computer which provided the dimensional change of the sample as a function of time and temperature.

#### d) Sintering

A Carbolite 1600°C (2912 °F) tube furnace was used to sinter the compacts in a controlled environment of 75% hydrogen and 25% nitrogen to avoid oxidation and contaminants. The bulk specimens were de-lubed at 400 °C (752 °F) to get rid of the stearic acid in order not to hinder the overall density and strength. Bulk samples from each milling hour were sintered at 900 °C (1652 °F) and 1120 °C (2048 °F) which is close to the critical sintering temperature of FC-0205 powder [31]. The temperature was set to ramp at 15 °/min and dwell for 30 minutes before it was slowly cooled to room temperature. The compaction and sintering schedule minimize grain growth and maximize densification during the process.

#### e) Microstructure Analysis and Sample Preparation

Struers LaboPress hot mounting technique was carried out on each sample for easy handling of the sample during grinding and polishing. Each surface of the mounted samples was subjected to grinding and polishing for proper analysis of the microstructure using SEM, optical microscopy (OM) and image analysis. The sintered samples were etched with 2% nitric acid and

78% ethanol to remove a uniform thin layer of the surface off for analysis of the grain size and grain growth. Zeiss Evo Supra 40 Field Emission Gun Scanning Electron Microscope FEG-SEM was used to analyze the morphology, particle distribution, grain size and agglomeration of milled and compacted FC-0205. Rikagu Ultima III x-ray diffraction system was used to analyze the average grain size of milled FC-0205. A thin layer of FC-0205 iron powder was evenly spread on a glass sample holder. This procedure was carried out on each powder sample of different milling time. The 2θ° (FWHM) range was set from 10° to 90° at 1°/min to cover the essential part of the powder pattern. ImageJ analysis was performed on images obtained from optical microscopy to analyze the extent of grain growth in the FC-0205 samples.

#### f) Hardness Test

Rockwell hardness (HRA) measurements using Leco Rockwell Hardness Tester were carried out on bulk specimens obtained through the compaction and sintering of FC-0205 steel powders. The indenter had a diamond cone shape for indenting. The indenter was forced into the material under a total load of 60 kgf. At least four different readings were taken from each surface of the sample, and the arithmetic average was obtained.

### III. MILLING, XRD, AND MICROSCOPY RESULTS

#### a) Ball Milling of Nanocrystalline Copper Steel Powders

Table 3 and Figure 2 shows analysis of FC-0205 particle size using particle size analyzer. A linear function relationship is obtained between milling time and average particle size of the copper steel powder. The linear function relationship is experimentally expressed in equation (2).

$$D = kt + 71.57 \quad (2)$$

Where D is the average particle size in (μm), t is the milling time in (hour) and k is a constant. The correlation coefficient of equation (2) is 0.998.

It was observed that as milling time of powder increased the average particle size decreased which agrees with previous studies [22,2] (see Table 3). As milling time increased from 0 to 16 hour, the rate of fragmentation of particles was high leading to a high reduction in particle size from 72.37 (μm) to 25.64 (μm). After further milling from 16 to 24 hours, it was noticed that fragmentation of particles decreased which led to a reduction in particle size from 25.64 (μm) to 3.7 (μm). The reduction in particle size is due to an increase in milling energy which causes an increase in the contact area between the grains.

Table 3: Milling time and average particle size

Milling Time (hours)	D <sub>50</sub> (μm)	% Decrease D50 (μm)	D <sub>90</sub> (μm)	Median Value (μm)
0	72.37	33.7709	165.6	82.23
8	47.93	46.50532	117.1	57.17
16	25.64	33.50234	76.95	26.05
20	17.05	78.29912	44.61	22.89
24	3.7	100	35.1	12.14

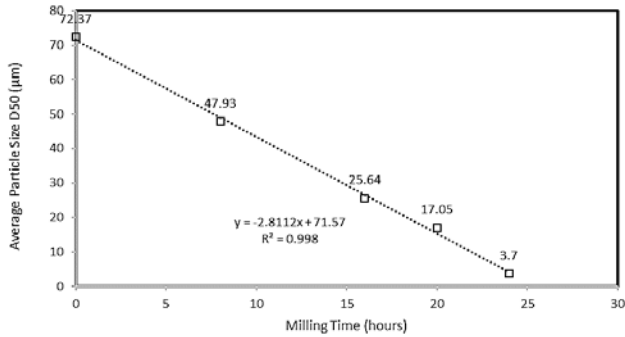
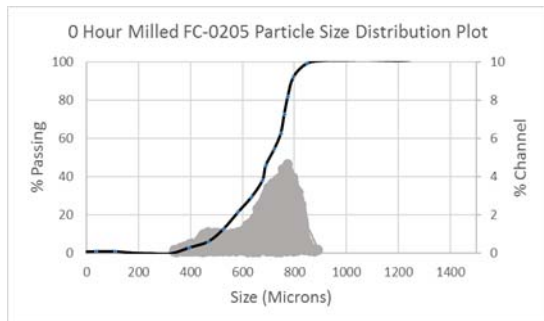
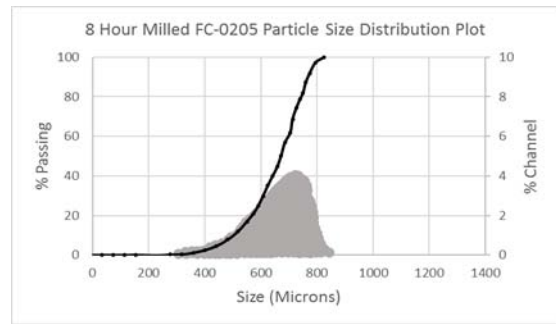


Figure 2: Milling Time vs. Average Particle Size

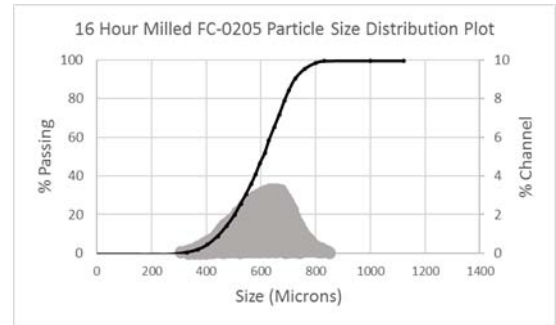
The particle size analysis experiments also offered information on the distribution of particle diameters in each sample. Figure 3 shows the particle size distribution plots for each powder analysis. For each successive increase in milling time, the peak of the distribution is seen to gradually skew from a right-sided distribution at 0-hour to a significantly left-sided distribution after 24 hours of milling with the peaks becoming narrower. The particle size distribution for the 8, 16, and 20-hour milled samples shows a mono-modal peak type compared to 0 (unmilled) and 24 milling hour which show a bi-modal peak type. The reason for the bi-modal peak could be as a result of higher particle size and coarser morphology of the 0 (unmilled) powder and high agglomeration obtained in the 24-hour milled powder. It was observed that at maximum peak for each milling distribution, the corresponding particle size decreased with increased milling time. For the unmilled powder, the average particle size is 72 (μm). In comparison, for the 24-hour milled powder, the average particle size is less than 5 (μm).



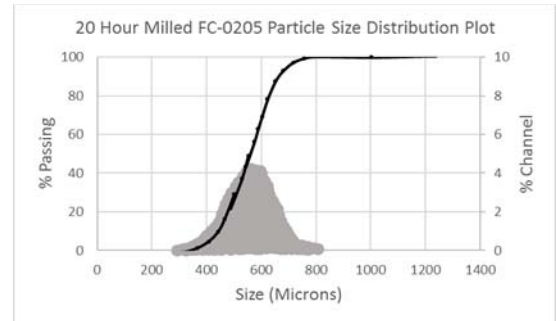
3(a)



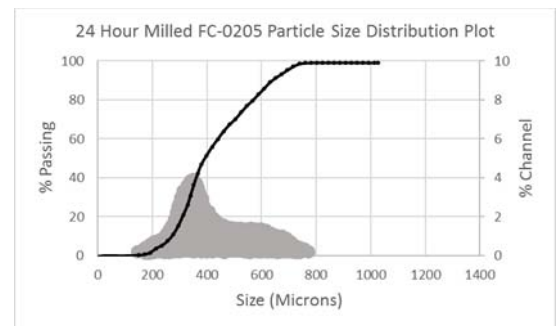
3(b)



3(c)



3(d)



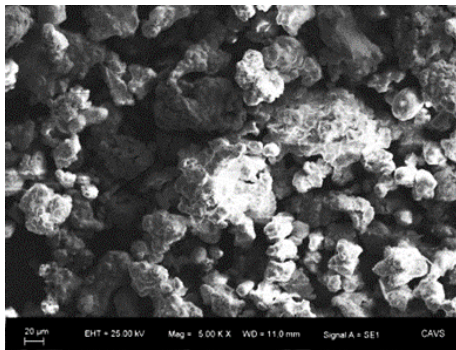
3(e)

Figure 3 (a-e): Particle size distribution plots of FC-0205 powder after milling durations of (a) 0 (un-milled), (b) 8, (c) 16, (d) 20, and (e) 24 hours

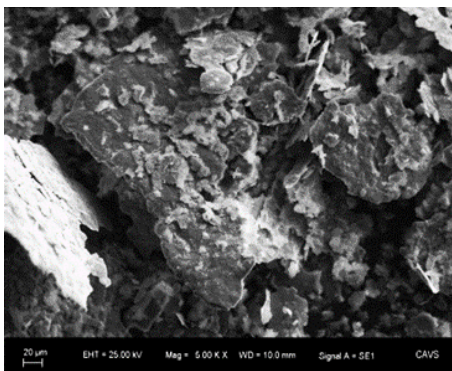
b) Scanning Electron Microscopy (SEM) of Copper Steel Powders

Scanning electron microscopy of the copper steel powder was performed to compare the morphology, agglomeration and particle size at different

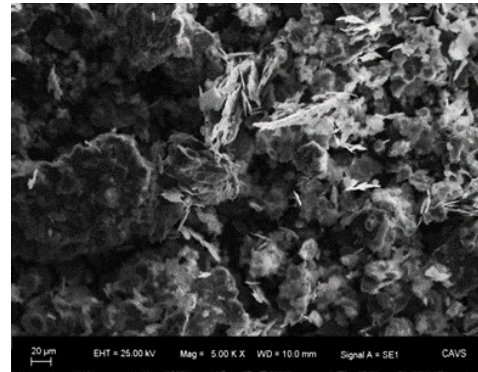
milling time and to determine the effect of particle size on consolidation. The SEM micrographs of the 0, 16, 20 and 24-hour milled copper steel powder at 5000X magnification is shown in Figure 4. It was observed that as milling time increased from 0 to 24-hour, the particle size became less coarse but was still in the micron meter range. However, higher agglomeration and morphology change of the steel powder was noticed as milling time increased. The morphology of the particle size for 0-hour (unmilled) powder is spherical as shown in Figure 4. As the milling time increased the particle size became flat and spongy with little agglomeration as shown in Figures 4 (b) and 4(c). The morphology change of the particles is due to an increase in milling energy which causes the contact area between grains to increase, as well as, an increase in the amount of coalesced particles, and a reduction in the plastic deformation of particles. The flat and spongy structure obtained due to increase milling time will be difficult to compact because of the high surface area which increases internal friction between particles. Hence, higher compaction pressure will be required to avoid high porosity and obtain high density. Increased agglomeration and a changes in morphology are also apparent in the 24-hour milled powder, as shown in Figure 4 (d). Increase in milling time causes more fracture of particles which results in further deformation and fragmentation of the steel particles.



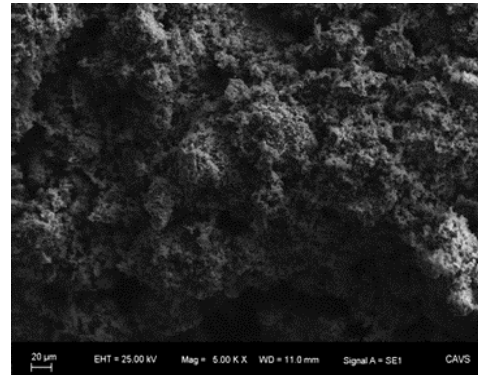
4(a)



4(b)



4(c)



4(d)

Figure 4 (a-d): Figure 4 SEM Images 5000X magnification of (a) (Unmilled) (b) 16 hour milled (c) 20 hour milled (d) 24 hour milled FC-0205 Powder respectively

#### c) X-Ray Diffraction of Copper Steel Powders

The results of the X-ray diffraction experiment, used to characterize the correlation between the grain sizes and milling time, are shown in Table 4 and Figure 7. It is empirically shown that a linear relation exists between grain size and milling time with a correlation coefficient of 0.998 as shown in equation (3).

$$L = -3.15t + 88.567 \quad (3)$$

where  $L$  is average grain size in (nm),  $t$  is milling time in (hour)

A linear reduction in grain size is obtained as milling time increases from 0 (unmilled) to 24-hour milled powder as shown in Figure 7. The X-ray diffraction peak patterns with angle  $2\theta$  values in the range from  $10^\circ$  to  $100^\circ$  for FC-0205 copper steel powders as shown in Figure 5. Figure 5 (a) shows a sharp diffraction line known as the full widths at half maximum (FWHM), which occurs in the micrometer range as shown in Table 4. However, as milling time increased, the diffraction line widths broadened, as shown in Figures 5 (b, c, and d) and grain decreased to the nanosize range as shown in Figure 6. The change noticed as a result of milling time is due to grain size refinement and increase in atomic level strains.

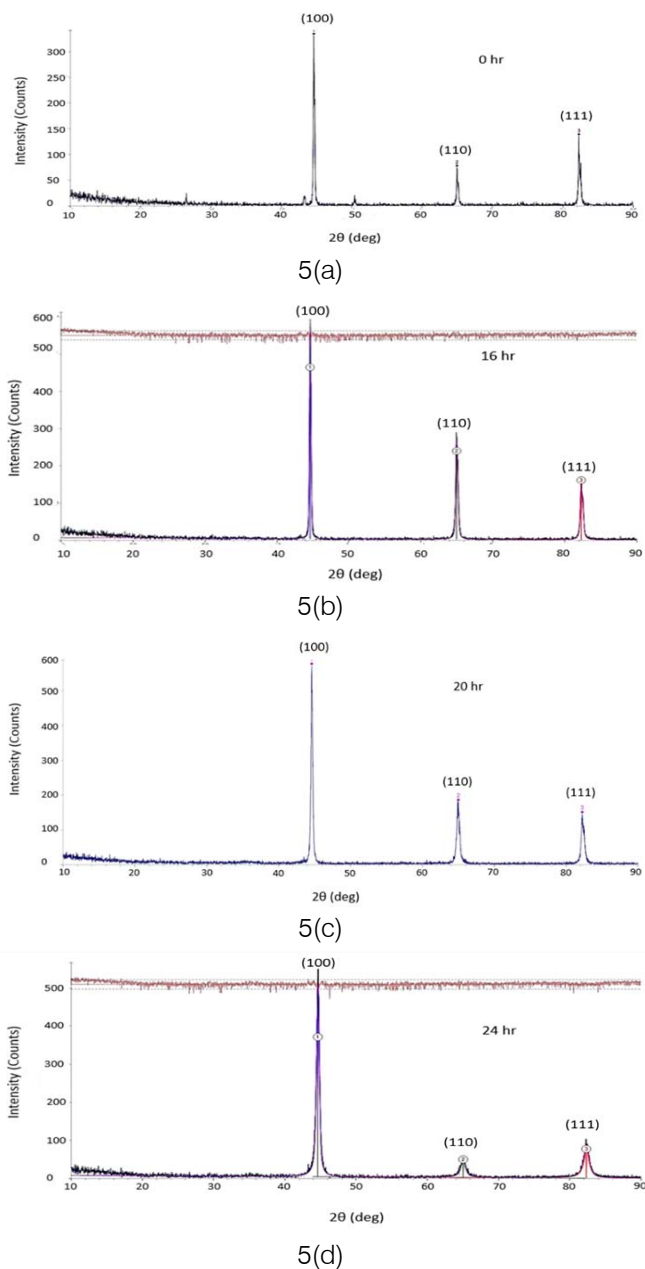


Figure 5: X-Ray diffraction peak profiles of milled powder samples at (a) 0 hour, (b) 16 hour, (c) 20 hour, (d) 24 hour.

Table 4: XRD result of average grain size for different milling times

Sample	Angle (°)	Centroid	Shape	FWHM (°)	Diameter (nm)
0Hr	64.961 (0.004)	1.4344Å	0.755v	0.145	>1000
16Hr	64.950 (0.004)	1.4347Å	0.495v	0.285	38.5
20Hr	64.934 (0.006)	1.4352Å	0.543v	0.412	24.9
24Hr	65.011 (0.012)	1.4342Å	0.880v	0.735	13.3

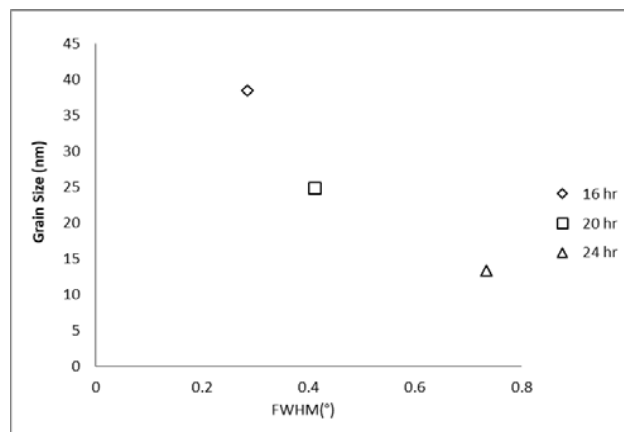


Figure 6: XRD Grain size vs. peak width

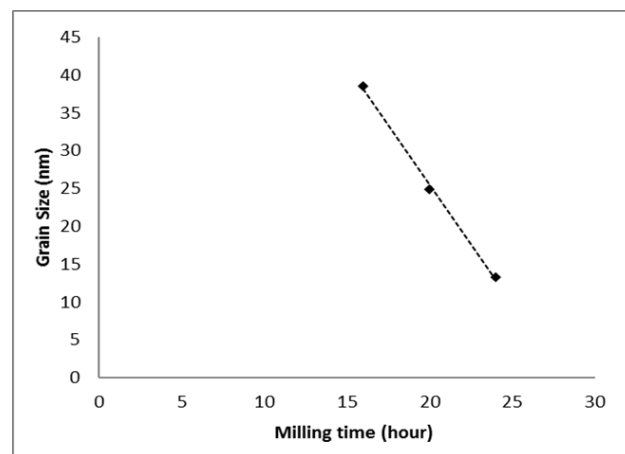


Figure 7: Grain Size vs. Milling Time

#### IV. COMPACTION AND SINTERING RESULTS

Figure 8 shows the variation in relative density of 0 (unmilled), 8 and 16-hour green compacts of FC-0205 powder as a function of compaction pressure. As pressure increased from 300 MPa, the 0-hour (unmilled) green compacts had higher relative density than 8-hour green compacts. Similarly, the 8-hour green compacts show a higher relative density when compared to the 16-hour green compacts. Thus, increased milling time of the powders resulted in decreased the density of the green compacts at a given pressure. The observation agrees with previous studies on copper steel powder [39]. It was observed that between 300 MPa to 400 MPa, 0-hour (unmilled) compacts show a higher relative density than 8-hour 16-hour compacts. Also, an insignificant difference in relative density between 0-hour and 8-hour green compacts is noticed. However as milling time increased to 16 hours, a significant drop in relative density is observed. The spongy structure that resulted from increased milling, hindered compaction. Therefore, higher compaction pressures are required to increase the density of the milled powder compacts.

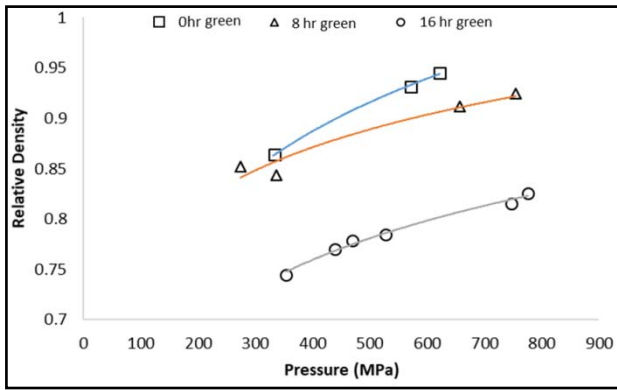


Figure 8: Compressibility Curve for 0, 8 and 16-hour milled FC-0205 powder

Figure 9 shows the rate of densification of 0 unmilled, 8 and 16-hour green compacts. The relationship between densification  $\ln(1/(1-D))$  and compaction pressure of the compacts show an elastic deformation property where particle sliding and rearrangement occur. A gradual increase in densification rate was noticed for unmilled compacts as compaction pressure increased. However, as milling time increased the densification rate decreased because of high frictional forces. Frictional force can be minimized by the addition of a moderate amount of lubricants which provide uniform flow during compaction. The densification function for 0-hour (unmilled), 8-hour 16-hour green compacts can be expressed as equations (4), (5) and (6), respectively.

$$\ln \left[ \frac{1}{(1-D)} \right] = KP + 0.96 \quad (4)$$

$$\ln \left[ \frac{1}{(1-D)} \right] = KP + 1.4 \quad (5)$$

$$\ln \left[ \frac{1}{(1-D)} \right] = KP + 1.1 \quad (6)$$

Where  $D$  is relative density,  $P$  is compaction pressure and  $K$  is a proportionality constant. The correlation coefficient of the equations is 0.99, 0.97 and 0.98 respectively.

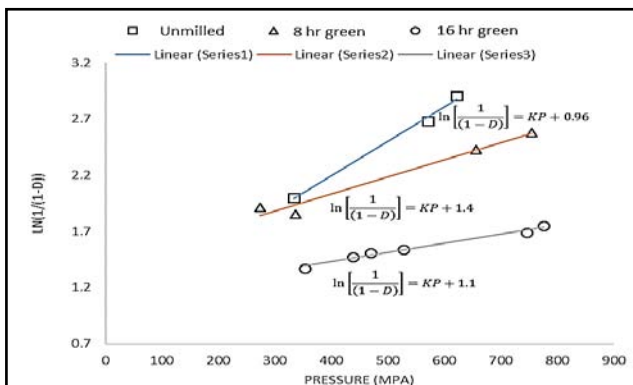


Figure 9: Figure 9  $\ln(1/(1-D))$  Vs Pressure

### a) Dilatometer tests

The resulting dimensional change from the dilatometer experiments for the unmilled FC-0205 compacts heated at 10 C/min, along with the corresponding temperature cycle is shown in Figure 10. The FC-0205 compact presents dimensional change after sintering due to the difference in alloy composition and powder size. As shown in Figure 10, the copper steel compacts experienced a thermal expansion of 0.7% at 700 °C (1292 °F). At this point, the iron ferrite, having a bcc structure, started to transform to austenite an FCC structure with some evidence of sample contraction. As temperature increased, carbon diffused into the austenite region. The copper in the sample began to melt at 1083 °C (1981 °F) which caused expansion of the compact. Near 1120 °C (2048 °F) all the copper melted and penetrated the austenite structure. During the 30 minutes hold time the sample started to contract again. As temperature decreased during uncontrolled cooling, copper precipitated from iron and austenite iron transformed into ferrite and pearlite (a mixture of  $\alpha$  ferrite and cementite  $Fe_3C$ ). After sintering the copper regions were no longer in the form of discrete particles, and the pearlite structure dominated the ferrite structure.

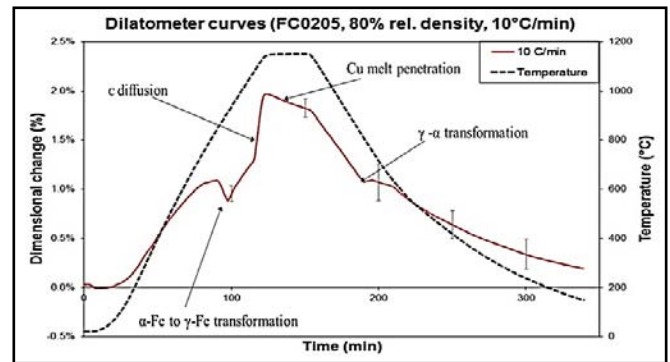


Figure 10: Dilatometer curves of dimensional change for the FC-0205 and FC-0208 at a heating rate of 10 °C/min.

The sintering behavior of the iron-copper-carbon system is very different compared to that of other PM metals. Figure 11 shows the typical shrinkage behavior during heating for nickel, 316L stainless steel, and bronze as compared to the expansion of the FC-0205 material during heating. The FC-0205 sample expanded to 1.5% at the maximum heating temperature 1150 °C (2102 °F). As the FC-0205 sample cooled, the material contracted, resulting in an overall dimensional change (shrinkage) of only 0.2% in the sample.

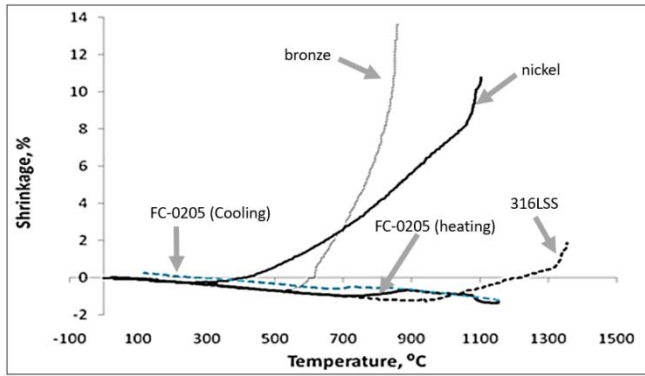


Figure 11: Comparison of sintering behavior of FC-0205, nickel, 316L stainless steel, and bronze

b) Sintering

FC-0205 copper steel powder samples were compressed to various heights to achieve different densities. Subsequently, the bulk samples were sintered at 900 °C (1652 °F) and 1120 °C (2048 °F) in a controlled nitrogen and hydrogen atmosphere to analyze density change with an increase in temperature. An insignificant difference in relative density was obtained between green compacts and bulk compacts sintered at 900 °C for 0 (unmilled) powder as shown in Figure 12. However, as milling time increased to 8 hours, a slight increase in relative density was noted between green compacts and compacts sintered at 900 °C (1652 °F) and 1120 °C (2048 °F) as shown in Figure 13. Figure 14 shows a significant increase in relative density with increased temperature for the 16-hour milled compacts. The increase in relative density is due to finer particles dissolving or diffusing into the base metal thereby creating a bonded final compact. Shrinkage during sintering can also be a factor due to a reduction in space and pores in the compact.

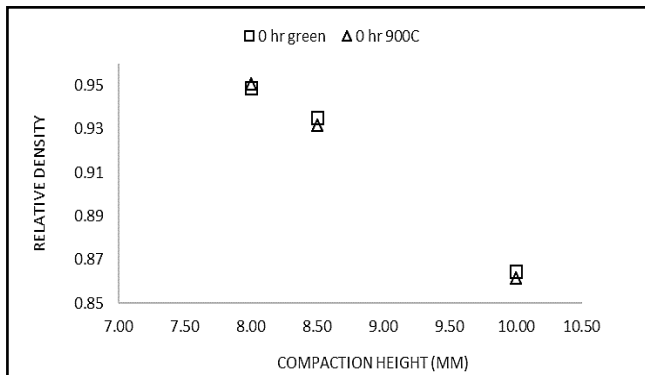


Figure 12: Relative density vs. compaction height for green and sintered (900 °C) unmilled compacts

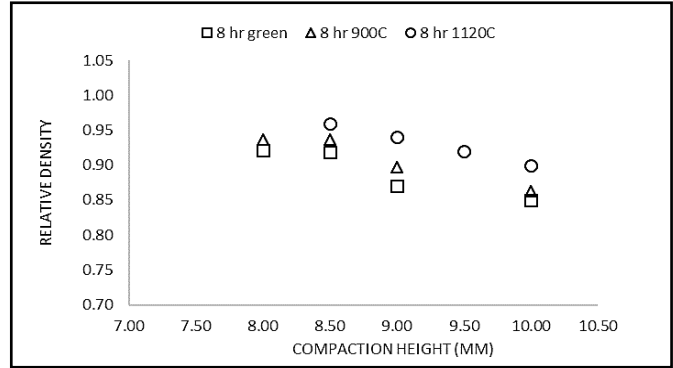


Figure 13: Relative density vs. compaction height for green and sintered (900 °C and 1120 °C) 8 hour milled powder compacts.

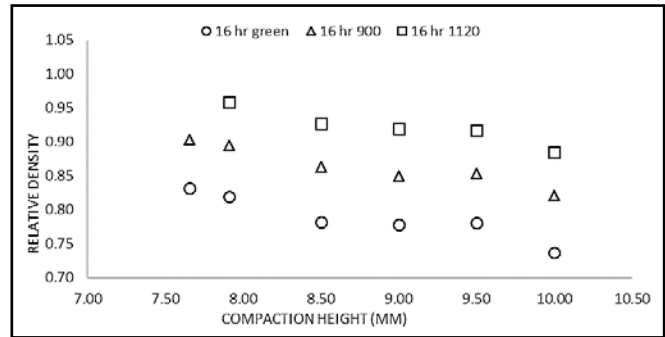


Figure 14: Relative density vs. compaction height for green and sintered (900 °C and 1120 °C) 16 hour milled powder compacts.

The microstructure in the 0-hour and 8-hour compacts sintered at 900 °C (1652 °F) show a better compaction and sintering of iron particles as shown in Figure 15 (b & d). Large pores are noticed in the 0-hour (unmilled) green compact as shown in Figure 15 (a) due to low compaction pressure. The large pores can affect the strength of the compact and act as a point of crack initiation which can lead to pre-mature fracture. High compaction pressure and sintering temperature can help control large porosity. Figure 15 (a) also shows elements and particles that are distinctly separated from each other, i.e., heterogeneous due to the unmilled powder of the green compact. The heterogeneous separation of particles allows the fine particles to fill in the inter-space between large particles, hence, increasing the powder packing and density of the green compact as obtained in the compressibility curve. The microstructure in 0 and 8-hour milled compacts sintered at 900 °C (1652 °F) show sinter bonding of powder particles and also the formation of pearlite as seen in Figure 15 (b and d). The shape, space and amount of pearlite depend on carbon diffusion and processing conditions. As temperature increases to 900 °C (1652 °F), iron ferrite transforms to austenite. As the sintering temperatures increase from 900 °C to 1120 °C (2048 °F), the diffusion of carbon into austenite takes

place, along with the formation of pearlite in 0 and 8-hour sintered compacts as shown in Figure 15 (c and e). Copper completely diffuses into austenite as temperature increases from 900 °C (1652 °F) to 1120 °C (2048 °F) for 0, 8 and 16 hour compacts. The diffusion of copper into iron austenite created some pores as shown in Figure 15 (c & e). Similarly, increase in sintering temperature of the compact causes phase change and grain redistribution. As temperature increases from 900 °C (1652 °F) to 1120 °C (2048 °F) for 0 and 8 hour compacts, phase change occurred from solid state phase to liquid state phase with the formation of high dominant pearlite in the microstructure as shown in Figure 15 (c & e). In the process of slow cooling, copper precipitate with the formation of pearlite and ferrite (cementite Fe<sub>3</sub>C) as shown in Figure 15 (c & e).

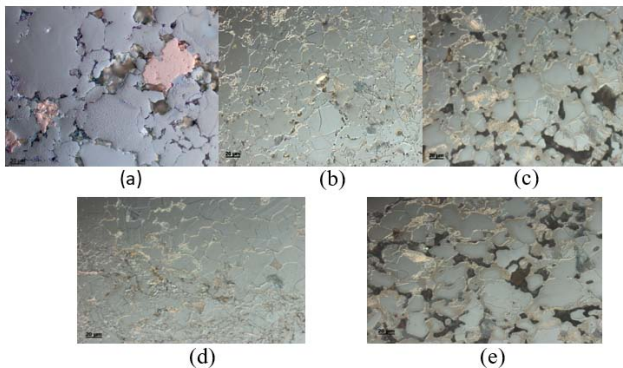


Figure 15: OM 500X magnification of (a) 0 (unmilled) green (b) 0 (unmilled) 900 °C (c) 0 (unmilled) 1120 °C (d) 8 hr 900 °C (e) 8 hr 1120 °C images showing grain size, grain distribution and voids of etched samples.

### V. MICROSTRUCTURE MEASUREMENT

The microstructural grains of FC-0205 sintered compacts were measured using ImageJ analysis free software according to ASTM standard E 112. The objective was to ascertain the extent of growth concerning sintering temperature. The sintered microstructure obtained from OM shows the variation of grain size distribution of copper steel compact in Figure 16 and also the image analysis grain size data in Table 5. As temperature increases to 900 °C (1652 °F), the formation of big and small microstructural non-uniform grain structures was noticed as seen in Figure 15 (b and d). Further increase in sintering temperature to 1120 °C (2048 °F) resulted in smaller grains coalescing to form a more uniform grain structure with pores due to copper diffusion into austenite iron as shown in Figure 15 (c and e). The increase in temperature resulted in grain size increase from 13.45 (μm) to 13.76 (μm) for 0-hour (unmilled) sintered compacts, similarly from 13.49 (μm) to 13.77 (μm) for 8-hour sintered compacts as obtained in Table 5. As temperature increased, grain growth is obtained as seen in Figure 16. Unmilled and 8-hour sintered compacts indicated little increase in grain size

and density as temperature increased from 900 °C (1652 °F) to 1120 °C (2048 °F). However, as temperature increased from 900 °C (1652 °F) to 1120 °C (2048 °F) in 16-hour sintered compacts, a significant increase in grain size and density is evident due to morphology and size of the powder.

Table 5: Average grain size

Sample	Relative Density (%)	Count	Total Area (nm <sup>2</sup> )	Average Size (μm)	%Area	Mean (μm <sup>2</sup> )	Mean Diameter (μm)
0hr-900C	0.92	284	54660.03	192.47	91.6	142.07	13.45
0hr-1120C	0.95	284	54789.03	192.92	90.82	148.62	13.76
8hr-900C	0.94	235	55422.57	235.84	92.18	142.87	13.49
8hr-1120C	0.95	283	54551.93	192.76	91.2	149	13.77
16hr-900C	0.91	380	54698.83	143.94	90.98	155.97	14.09
16hr-1120C	0.92	211	55683.8	263.9	92.62	173.66	14.87

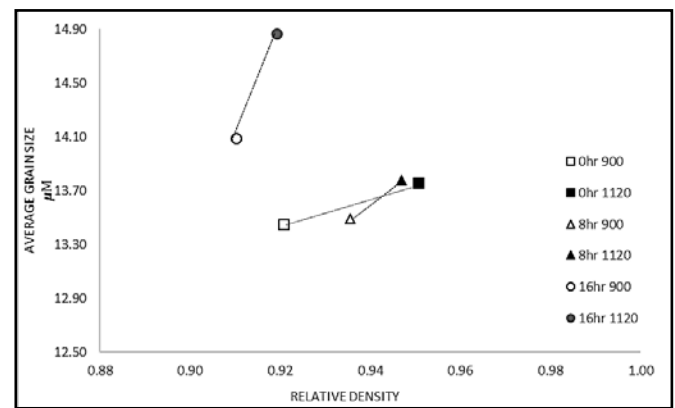


Figure 16: Average grain size vs. relative density for 0,8 and 16-hour milled powder compacts sintered at 900 °C and 1120 °C. grain size, grain distribution and voids of etched samples.

#### a) Hardness Test

Table 6 shows the mechanical properties obtained for FC-0205 copper steel powder using Rockwell hardness test at a maximum load of 60 kg. Four separate tests were performed on each sample, and the average was obtained for proper analysis of the strength. Each sample was polished to avoid spatial variability in hardness. It was noticed that Rockwell hardness for each milling hour increased as temperature increased, demonstrating the impact of sintering temperature on compact strength. However, Rockwell hardness for the 0-hour (unmilled) and 8-hour compacts was relatively close, but a significant difference was observed in the 16-hour compacts as temperature increased. Increase in density increased hardness of the sintered compacts as shown in Figure 17 and Table 7. Also, in Table 7, the 16-hour compacts show lower mechanical properties as regards to the density and hardness than the 0 (unmilled) and 8 hour sintered compacts. The reduced mechanical properties of the 16-hour compacts are due to the fine particle structure of the powder which makes compaction difficult and

possible formation of pores in the compacts. It is observed that the finer the particle size of the powder, the more difficult to compress, hence lower strength is obtained.

Table 6: Rockwell Hardness results for sintered compacts

Sample	1	2	3	4	Average (HRA)
0hr 900	31.9	30.8	27.7	27.3	29.43
0hr 1120	32.2	29.5	32.4	31.4	34.88
8hr 900	34.4	32.6	32.1	31.8	32.73
8hr 1120	35.1	34.9	34	33.8	34.45
16hr 900	16.1	17.9	18.4	16.9	17.33
16hr 1120	22.2	22.8	20.3	21.6	21.73
Method	Rockwell Hardness HRA				
Indentor	Diamond cone				
Total Load	60kgf				

Table 7: Hardness, relative density, and grain size relationship

Sample	Relative Density	Average HRA (kGF)	Mean Daimeter (um)
0hr 900	0.921	29.43	13.45
0hr 1120	0.951	34.88	13.76
8hr 900	0.936	32.73	13.49
8hr 1120	0.947	34.45	13.77
16hr 900	0.91	17.33	14.09
16hr 1120	0.919	21.73	14.87

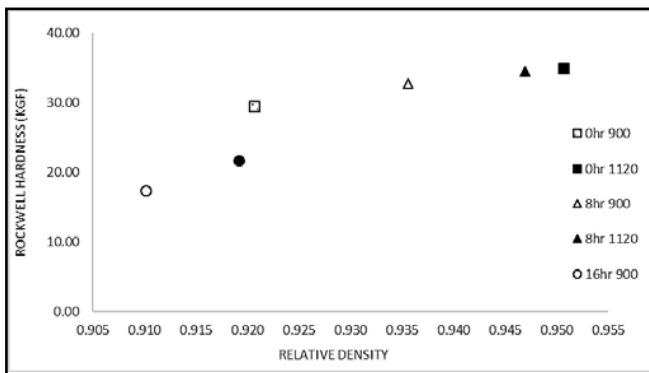


Figure 17: Hardness vs. Relative density

## VI. CONCLUSION

This experimental study establishes a correlation between milling time, particle size, temperature and grain growth through HEBM on copper steel powder. Results from this study agrees with previous studies which show that increased milling time of powder particles decreased the average particle size as well as grain size due to high rate of particle fragmentation. Although at higher milling time,

fragmentation rate was low resulting in low reduction in particle size. The particle size reduction rate was as a result of higher milling energy which increases the contact areas between grains, therefore, welding of particles is obtained. Particle size analysis showed distribution peaks that was getting narrower and also skewing from right to left due to increased milling time of the copper-steel powder. The increase in milling time caused change in morphology and higher agglomeration of the powder particles. The change in morphology noticed with increased milling can hinder compaction because of high surface area that increases internal friction between particles. Therefore, higher compaction pressure will be required to achieve a good dense compact. A linear reduction in grain size was obtained as milling time increased. As pressure was increased in green compacts, density also increased. It was noticed that at the same pressure range, lower milling hour compacts obtained higher density. Therefore higher compaction pressure is required for higher milling hour to avoid a high porous compact. Contraction of copper steel compact was noticed at 700 °C (1292 °F) as the microstructure transformed from iron ferrite to iron austenite. Further increase in temperature to 1083 °C (1981 °F) resulted in copper melting into iron austenite which led to expansion of the compacts. It was observed that increase in milling time between 0 (unmilled) and 8 hour compacts showed a slight increase in relative density as temperature increased to 1120 °C (2048 °F). A significant increase in relative density was obtained for 16 hour compacts at the same temperature. Hence, higher milling time and higher temperatures resulted in increased density of the compacts. increases the density of the compacts at the same temperature increase. However, grain growth was significant in the 16-hour milled compacts as temperature was increased during sintering as compared to the 0 (unmilled) and 8 hour compacts sintered at the same temperature. As compared to the 0-hour and 8-hour milled and sintered samples, the 16-hour milled, sintered compacts The finer sized powders require higher compaction pressure to increase pre-sintering density and reduced sintering temperature to prevent grain growth.

## REFERENCES RÉFÉRENCES REFERENCIAS

1. Nieman G.W, Weertman, J.R., Siegel, R.W., 1991 "Mechanical behavior of nanocrystalline Cu and Pd" Journal of Material Research 6 (5).
2. Akhtar S.Khan, Yeong S. Suh, Xu Chen, Hayoyue Zhang, Laszlo Takacs " Nanocrystalline Aluminum: Mechanical Behavior at Quasi-Static and high strain rates, and constitutive modeling" (2006) 195-209.
3. C. Suryanarayana. "The Structure and Properties of Nanocrystalline Materials" Issues and Concerns. JOM (September 2002).

4. T.G.Nieh, P.Luo, W.Nellis, D.Lesuer, D.Benson. *Acta Mat.* 44 No. 9 (1996) 3781-3788.
5. Sanders, P.G., Eastman, J.A., Weertman, J.R., 1996. "Tensile behavior of nanocrystalline Cu the Minerals" *Metals and Materials Society*, pp. 379-386.
6. G.Dieter. *Mechanical Metallurgy* 3<sup>rd</sup> Edition 1986.
7. Neils Hansen, "Hall-Petch relation and boundary strengthening" *Hansen Scripta Materialia* 51 (2004) 801-806.
8. K.S. Kumar, H.V. Swygenhoven, S.Suresh. *Acta Materialia* 51 (2003) 5743-5774.
9. M. Furukawa, Z. Horita, M. Nemoto, R. Z. Valiev, T. G. Langdon. *Acta Mater*, Vol. 44, pp. 4619- 4629. 1996.
10. S.C.Tjong, Haydn Chen," *Nanocrystalline Materials and coatings*," R45(2004) 1-88.
11. M. A Meyers, A.Mishra, D.J Benson. "Mechanical properties of nanocrystalline materials" *Progress in Materials Science* 51 (2006) 444.
12. H.Conrad, J.Narayan. "On the grain size softening in nanocrystalline materials" *Scripta Mater* 42 (2000) 1025-1030.
13. E. Bonetti, L. Pasquini, E. Sampaolesi "The influence of grain size on the mechanical properties of nanocrystalline Aluminum," Vol 9 (1997) 611-614.
14. K.S. Kumar, H.V. Swygenhoven, S.Suresh. *Acta Materialia* 51 (2003) 5743-5774.
15. Brian W. James "Powder Metallurgy Methods and Applications" Vol 7, *Powder Metallurgy*.
16. Alymov M. I, Maltina E. I, and Stephanov Y. N, *Powder Metal Technology and Applications*, Vol 7, *ASM Handbook*, American Society for Metals, 1998, p 506.
17. Akhtar S.Khan, Hayoyue Zhang, Laszlo Takacs "Mechanical response and modelling of fully compacted nanocrystalline iron and copper" (2000) 1459-1476.
18. Edelstein, A.S., Cammarata, R.C. "In Nanomaterials: Synthesis, Properties and Applications". Institute of Physics Publishing, Bristol and Philadelphia, 1996.
19. Joao Fogagnolo, Elisa Ruiz-Navas, Maria Robert, Jose Torralba "The Effects of Mechanical Alloying on the Compressibility of Aluminum Matrix Composite Powder" (2003) 50-55.
20. H. J. Fecht, E. Hellstern, Z. Fu, and W. L. Johnson, "Nanocrystalline metals prepared by high-energy ball milling," *Metall. Trans. A*, vol. 21 2333-2337, Sep. 1990.
21. Suryanarayana C, Ivanov E, Boldyrev V "The Science and Technology of Mechanical Alloying" (2001) 151-158.
22. D. Poquillon, V. Baco-Carles, Ph. Tailhades, E. Andrieu "Cold compaction of iron powders relations between powder morphology and mechanical properties" (2002) 75-84.
23. R. M. German "Strength Dependence on Porosity for P/M Compacts" *Int. J. Powder Met. Powder Tech.* 1977 Vol. 13, 259-271.
24. R. Haynes "Fatigue behavior of sintered metal and alloys" *PM* 1970 Vol. 13 No 26.
25. T. Honda "Effect of sintering Temperature and Time on Fatigue Strength of Iron Compacts with Different Particle Sizes." *J. Jpn. Soc. Powder Powder Metall.* 1983 Vol. 30, 273-277.
26. C.E. Carlton, P.J. Ferreira. *Acta Materialia*, 55 (2007) 3749-3756.
27. Pranav G, Seong-Jin P, Randall M "Effect of Die Compaction pressure on Densification Behavior of Molybdenum Powders" (2007) 16-24.
28. Vagnon A, Lame O, Bouvard D, Di Micheal M, Bellet D, Kapelski G "Deformation of Steel Powder Compacts during Sintering: Correlation between Macroscopic Measurement and in Situ Microtomography Analysis" (2006) 513-522.
29. Montasser Dewidar, G.T. Abdel-Jaber, Mahmoud Bakreya, and Hussien Badry "Effect of Processing Parameters and amount of additives on the Mechanical Properties and Wear Resistance of Copper-based Composite" *IJMME-IJENS* Vol. 10 2013.
30. Sang Ho Na, Si Hyung Kim, Young-Woo Lee and Dong Seong Sohn "Effect of Ball-Mill Treatment on Powder Characteristics, Compaction and Sintering Behaviors of ex-AUC and ex-ADU UO Powder" (2002) 60-67.
31. Camila Dos Santos Torres & Lirio Schaffer "Effect of High Energy Milling on the Microstructure and Properties of WC-Ni Composite" (2010) 293-298.
32. Ravi K. Enneti, Adam Lusin, Sumeet Kumar, Randall M. German, Sunday V. Atre "Effects of Lubricant on Green Strength, Compressibility and Ejection of Parts in Die Compaction process" (2013) 22-29.
33. M. Ward & J.C Billington "Effect of Zinc Stearate on Apparent Density, Mixing and Compaction /Ejection of Iron Powder Compacts" *Powder Metallurgy* Vol. 22 Issue 4, 1979.
34. K.S Narasimhan "Sintering of Powder mixtures and the growth of ferrous powder metallurgy" (2001) 56-65
35. German R. M "Sintering Theory and Practice" New York: John Wiley and Sons; 1996.
36. R R.M. German "The Sintering of 304L Stainless Steel" *Metallurgical Transactions* Vol. 7A Dec 1976 1879-1885.
37. Babak Farrokh, Akhtar Khan "Grain Size, Strain Rate, and Temperature Dependence of Flow Stress in Ultra-Fine grained and Nanocrystalline Cu and Al: Synthesis, Experiment, and Constitutive Modeling" (2009) 715-732.
38. *Powder Metal Technology and Applications*, Vol 7, *ASM Handbook*, American Society for Metals, 1998, p 77.

39. In-Hyung Moon & Kyung-Hyup Kim "Relationship between compacting pressure, green density, and green strength of copper powder compacts" Powder Metallurgy Vol 27, Issue 2, pages 80-84 1984